Pergamon

SCIENCE DIRECT

Bioorganic & Medicinal Chemistry Letters 13 (2003) 2967–2971

BIOORGANIC & MEDICINAL CHEMISTRY LETTERS

Identification of a New Chemical Class of Potent Angiogenesis Inhibitors Based on Conformational Considerations and Database Searching

Pascal Furet,[a,*] Guido Bold,[a] Francesco Hofmann,[a] Paul Manley,[a] Thomas Meyer[a] and Karl-Heinz Altmann[b]

[a]*Oncology Research, Novartis Pharma AG, CH-4002 Basel, Switzerland*
[b]*Corporate Research, Novartis Pharma AG, CH-4002 Basel, Switzerland*

Received 22 January 2003; accepted 17 March 2003

Abstract—The vascular endothelial growth factor (VEGF) tyrosine kinase receptors KDR and Flt-1 are targets of current interest in anticancer drug research. PTK787/ZK222584 is a potent inhibitor of these enzymes in clinical evaluation as an antiangiogenic agent. The development of a hypothesis concerning the bioactive conformation of this compound has led to the discovery of a new class of potent inhibitors of KDR and Flt-1, the anthranilamides. This could be achieved with a limited experimental effort, which only involved the testing of one archive compound and the synthesis and testing of one appropriate analogue.

Introduction

Inhibition of tumor induced angiogenesis is a promising strategy in anticancer drug research.[1,2] Selective inhibition of the tyrosine kinase enzymatic activity of the two vascular endothelial growth factor (VEGF) receptors KDR and Flt-1 is an approach[3–7] we are pursuing in this area.

In this respect, we have previously reported the discovery of the anilinophthalazine compound PTK787/ZK222584 (**1**), a potent and selective inhibitor of the kinase activity of KDR and Flt-1, which is currently undergoing clinical evaluation.[8,9] More recently, we have disclosed anthranilic acid amide derivatives, which represent a novel chemical class of inhibitors of these enzymes, with promising in vivo antitumor effects.[10] In this article, we describe how, following a line of reasoning based on a conformational analysis of **1**, this new class of angiogenesis inhibitors was discovered.

Conformational Analysis of Compound 1

As **1** was identified by high-throughput screening and not by structure-based design or pharmacophore modeling, the structural and conformational determinants of its kinase inhibitory activity were completely unknown initially. As part of our efforts to elucidate these, we undertook a conformational analysis of the inhibitor by computational methods.[11]

This analysis provided a set of 24 energy-minimized conformations that could be classified in two subsets corresponding, respectively, to an *anti* and a *syn* orientation of the anilino N–H bond with respect to the C1–N2 bond of the phthalazine nucleus as depicted in Figure 1. *anti* conformations were on average 3.0 kcal/mol more stable than the *syn* conformations reflecting the partial deconjugation of the aniline and phthalazine moieties occurring in the latter because of steric hindrance between the chlorophenyl ring and the phthalazine benzenoid cycle. This was confirmed by ab initio calculations on the smaller model compound lacking the methylpyridyl part which indicated a destabilization of the *syn* conformation by 3.1 kcal/mol compared to its *anti* counterpart.

*Corresponding author. Tel.: +41-61-696-7990; fax: +41-61-696-6246; e-mail: pascal.furet@pharma.novartis.com

0960-894X/03/$ - see front matter © 2003 Elsevier Ltd. All rights reserved.
doi:10.1016/S0960-894X(03)00626-7

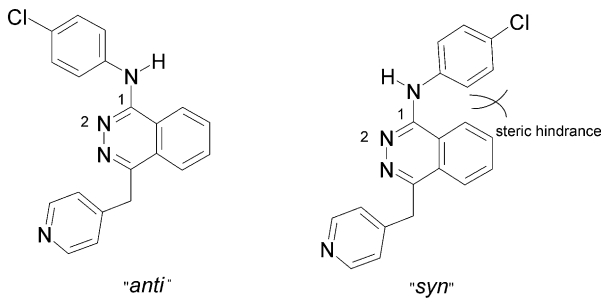

Figure 1. Two possible orientations of the aniline moiety with respect to the phthalazine nucleus in **1**.

Implication for the active conformation

Database searching. The numerous available X-ray crystal structures of inhibitor–kinase complexes show the conservation of a hydrogen bonding interaction between the inhibitor and the backbone of the protein in the so called 'hinge' region.[12,13] The hinge region corresponds to the amino acid stretch that connects the N- and C-terminal domains of the kinase whose interface forms the ATP (cofactor) binding site. Inhibitors often achieve hydrogen bonding to the hinge region by means of a bidentate donor–acceptor system present in their structure.[14–16] One can recognize such a hydrogen bond donor–acceptor system in **1** (the anilino NH group and the phthalazine N2 atom) when the inhibitor is represented in a *syn* conformation (see Fig. 1). However, as shown by our conformational analysis, the *syn* conformations are of high energy. **1** is thus unlikely to adopt a *syn* conformation upon binding to an enzyme pocket. A potent bioactive compound is not expected to bind to a protein in a conformation that is significantly less stable than its predominant conformation in solution.[17] To be highly active, a compound must avoid wasting a large part of the free energy stabilization gained by forming favorable interactions with the protein and desolvating hydrophobic groups for conformational adaptation.

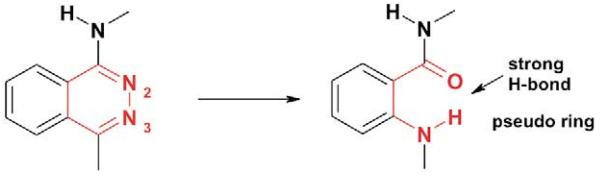

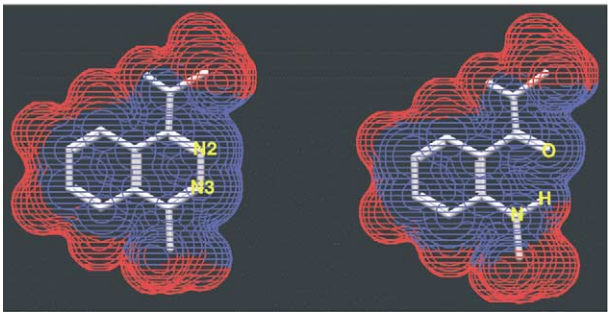

Figure 2. Van der Waals surface/molecular electrostatic potential representations of the phthalazine moiety of **1** (left) and its anthranilic acid amide mimetic (right). The potential isovalue contour lines appear in red for positive values and in blue for negative ones.

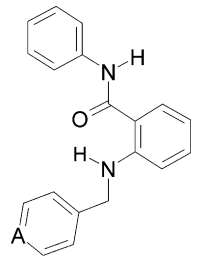

Figure 3. Substructure query used in the database search.

This led us to assume that the KDR/Flt-1 inhibitory conformation of **1** is of the *anti* type with the consequence that the anilino NH group and the phthalazine N2 atom do not correspond to the hydrogen bond donor–acceptor system interacting with the hinge region present in many kinase inhibitors. This hypothesis prompted us to further investigate the role played by the different parts of the inhibitor in its KDR/Flt-1 inhibitory activity. We were particularly interested to investigate the importance of the phthalazine nitrogen atoms.

To this end, we conducted a series of substructure searches in the Novartis collection of compounds with the aim of retrieving analogues or mimetics of **1** lacking one or two of the phthalazine nitrogen atoms for subsequent KDR/Flt-1 testing. In one of these searches, we reasoned that an anthranilic acid amide moiety presenting a strong intramolecular hydrogen bond between the amine and keto functionalities[18] could mimic the phthtalazine ring of **1** by formation of a pseudo six-membered ring. As illustrated in Figure 2 by van der Waals surface/electrostatic potential representations,[19] such a moiety can mimic the phthalazine ring in all respects but the possibility of potential N3 hydrogen bonding. Thus, with this mimic we could probe the importance of the phthalazine N3 atom for KDR/Flt-1 inhibitory activity. The Novartis compound collection was consequently searched using the substructure query shown in Figure 3. The search returned a single compound available for testing: **2**. Interestingly, this compound turned out to inhibit KDR and Flt-1 with IC_{50} values of 3.7 and 23 μM, respectively, as reported in Table 1.[20]

Table 1. IC_{50} (μM) values[a] of compounds **1**–**3** in kinase assays

Kinase	**1**[b]	**2**	**3**
KDR	0.037	3.7	0.020
Flt-1	0.077	23	0.18
c-Kit	0.73	—	0.24
EGF-R	> 10	—	7.3
CDK-1	> 10	—	> 10
c-Met	> 10	—	> 10
IGF-1R	> 10	—	> 10
c-Src	> 10	—	7.0
PKA	> 10	—	> 10

[a]The data represent averages of at least three determinations.
[b]Data from ref 9.

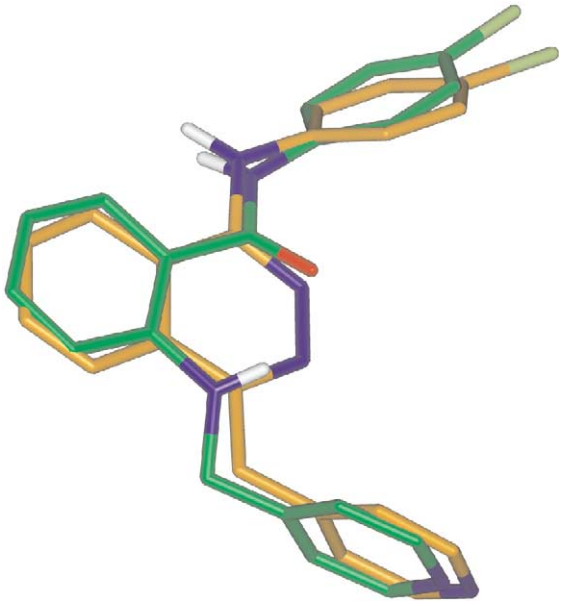

Figure 4. Superposition of the calculated lowest-energy conformations of **1** and **3**.

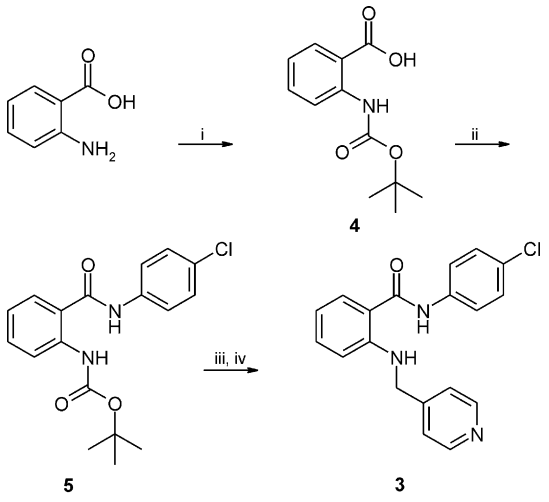

Scheme 1. (i) BOC_2O, NEt_3, DMF, rt, 16 h, 59%; (ii) 4-chloro aniline, HBTU, NMM, DMF, rt, 16 h, 35%; (iii) 4 N HCl/dioxane/MeOH 7.5/1, rt, 3.5 h, 98%; (iv) pyridine-4-carbaldehyde, $NaCNBH_3$, MeOH/AcOH 100/1, rt, 2 h, 33%.

Synthesis of a potent mimetic. The finding that **2** possessed significant KDR and Flt-1 inhibitory activity prompted us to synthesize **3**, the exact anthranilic amide mimetic of **1** in which the *para*-fluoro and *ortho*-fluoro substituted phenyl rings of **2** are replaced by a 4-pyridyl moiety and a *para*-chloro substituted phenyl, respectively. In the series of **1**, a *para*-chloro substituent on the phenyl ring of the aniline moiety is clearly beneficial.[21]

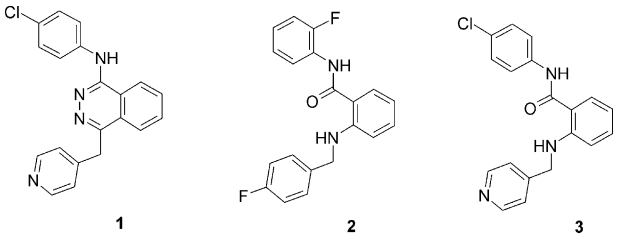

When tested, **3** showed a dramatic increase in KDR/Flt-1 inhibitory activity relative to **2**, resulting in a compound with the same level of potency and selectivity[22] as **1** (Table 1), thus validating the mimetism concept. With **3**, we had an entry in a new class of potent inhibitors of KDR and Flt-1. The high activity of this compound also shed some light on the structural determinants of the potency of **1**. As discussed above, it meant that the phthalazine N3 atom is probably not engaged in hydrogen bonding with KDR or Flt-1 and therefore a polar atom at this position might not be required for activity. Moreover, it gave support to the hypothesis that the active conformation of **1** is of the *anti* type. An active *syn* conformation for **1** would imply an active conformation of **3** in which the amide group adopts an improbable high energy *cis* conformation. An overlay of the calculated lowest energy conformational minima of **1** and **3** is shown in Figure 4.

Chemistry

The synthesis of compound **3** is summarized in Scheme 1.[23] Anthranilic acid was converted to its BOC-protected derivative **4**,[24] which upon HBTU activation was reacted with *p*-chloro aniline to provide anilide **5**.[25] Following removal of the BOC-protecting group with 4 N HCl/dioxane, reductive amination of the resulting amine **6**[26] with pyridine-4-carbaldehyde in the presence of $NaCNBH_3$ gave the desired compound **3**[27] as white crystals in 33% yield.

Conclusion

As the result of an investigation aimed at understanding the conformational and structural basis of the KDR/Flt-1 inhibitory activity of **1**, we identified a new class of inhibitors of these enzymes that possess potent anti-angiogenic and antitumor properties.[10] In the era of high throughput approaches to drug discovery, where it is believed that the screening or synthesis of very large numbers of compounds are required, the work reported here illustrates that large scale experimental effort is not the only way to tackle the difficult problem of identifying active compounds of pharmacological interest. With a structure-based reasoning that led to the testing of one archive compound and the synthesis of only one analogue, we were able to discover a novel inhibitor chemotype for important target enzymes in anticancer drug research.

References and Notes

1. Matter, A. *Drug Discov. Today* **2001**, *6*, 1005.
2. Kerbel, R. S. *Carcinogenesis* **2000**, *21*, 505.
3. Sun, L.; McMahon, G. *Drug Discov. Today* **2000**, *5*, 344.
4. Manley, P. W.; Furet, P. In *Anticancer Agents: Frontiers in Cancer Chemotherapy*; Ojima, I., Vite, G., Altmann, K., Eds.; ACS Symposium Series 796; American Chemical Society: Washington, DC, 2001; p 282.
5. Veikkola, T.; Karkkainen, M.; Claesson-Welsh, L.; Alitalo, K. *Cancer Res.* **2000**, *60*, 203.

6. Boyer, S. J. *Curr. Top. Med. Chem.* **2002**, *2*, 973.
7. Adams, J.; Huang, P.; Patrick, D. *Curr. Opin. Chem. Biol.* **2002**, *6*, 486.
8. Bold, G.; Altmann, K.-H.; Frei, J.; Lang, M.; Manley, P. W.; Traxler, P.; Wietfeld, B.; Brueggen, J.; Buchdunger, E.; Cozens, R.; Ferrari, S.; Furet, P.; Hofmann, F.; Martiny-Baron, G.; Mestan, J.; Roesel, J.; Sills, M.; Stover, D.; Acemoglu, F.; Boss, E.; Emmenegger, R.; Laesser, L.; Masso, E.; Roth, R.; Schlachter, C.; Vetterli, W.; Wyss, D.; Wood, J. M. *J. Med. Chem.* **2000**, *43*, 2310.
9. Bold, G.; Frei, J.; Furet, P.; Manley, P. W.; Bruggen, J; Cozens, R.; Ferrari, S.; Hofmann, F.; Martiny-Baron, G.; Mestan, J.; Meyer, T.; Wood, J. M. *Drugs Future* **2002**, *27*, 43.
10. Manley, P. W.; Furet, P.; Bold, G.; Brüggen, J.; Mestan, J.; Meyer, T.; Schnell, C. R.; Wood, J.; Haberey, M.; Huth, A.; Krüger, M.; Menrad, A.; Ottow, E.; Seidelmann, D.; Siemeister, G.; Thierauch, K.-H. *J. Med. Chem.* **2002**, *45*, 5687.
11. The conformational analysis of **1** was performed in Macromodel[30] using the Monte-Carlo/energy minimization method (automatic set up-standard protocol) and the AMBER* force field in conjunction with the GB/SA water solvation model. The ab initio calculations (restricted Hartree–Fock) were performed in Gaussian 92 using the 3-21G basis set and full geometry optimization.
12. Toledo, L. M.; Lydon, N. B.; Elbaum, D. *Curr. Med. Chem.* **1999**, *6*, 775.
13. Traxler, P.; Furet, P. *Pharmacol. Ther.* **1999**, *82*, 195.
14. Furet, P.; Meyer, T.; Strauss, A.; Raccuglia, S.; Rondeau, J. M. *Bioorg. Med. Chem. Lett.* **2002**, *12*, 221.
15. Zhu, X.; Kim, J. L.; Newcomb, J. R.; Rose, P. E.; Stover, D. R.; Toledo, L. M.; Zhao, H.; Morgenstern, K. A. *Structure* **1999**, *7*, 651.
16. Mohammadi, M.; Froum, S.; Hamby, J. M.; Schroeder, M. C.; Panek, R. L.; Lu, G. H.; Eliseenkova, A. V.; Green, D.; Schlessinger, J.; Hubbard, S. R. *EMBO J.* **1998**, *17*, 5896.
17. Bostrom, J.; Norrby, P.-O.; Liljefors, T. *J. Comput.-Aided Mol. Des.* **1998**, *12*, 383.
18. A search of the Cambridge crystallographic database using the anthralinic acid amide moiety shown in Figure 3 as substructure query returned 14 X-ray crystal structures of small organic molecules presenting this motif. In all of them, an intramolecular hydrogen bond between the amine and keto functionalities was present. Representative structures of this type have the following entry codes in the database: YEGWUC, YEGWOW, TIDNAV and MAMBIL. Ab initio calculations using the 3–21 G basis set indicate that the global conformational minimum of the molecular fragment shown on the right hand side of Figure 2 is the conformer presenting the intramolecular hydrogen bond. The next conformational minimum is less stable by around 5 kcal/mol.
19. In Figure 2, the molecular electrostatic potential displayed as isovalue contour lines on the van der Waals surface[31] was calculated using the Coulomb formula with atomic point charges. These were obtained in MOPAC (version 6.0)[32] by fitting the molecular electrostatic potential calculated from a wavefunction in the MNDO approximation.
20. Enzyme Inhibition Assays. For the tyrosine kinases, inhibition assays were performed as filter binding assays using recombinant GST-fused kinase domains of the receptors expressed in baculovirus and purified over glutathione sepharose. [^{33}P]-ATP was used as the phosphate donor and the polyGluTyr (4:1) peptide was used as the acceptor (for details see ref 8). The CDK1 and PKA assays are described in refs 28 and 29, respectively. Assays were performed under conditions optimized for each kinase and with ATP concentrations similar to the K_m of the respective enzyme towards ATP: 8.0 μM (KDR, Flt-1), 1.0 μM (c-Kit, c-Met), 2.0 μM (EGF-R), 20 μM (c-Src), 30 μM (IGF-1R), 7.5 μM (CDK1) and 50 μM (PKA).
21. A comparison of he KDR inhibitory activity of the first two compounds reported in Table 3 of ref 8 shows the beneficial effect of this chlorine atom.
22. **3** like **1** is a potent inhibitor for KDR, Flt-1 and kinases of the PDGF-R family like c-Kit. It is inactive on kinases of the AGC family (PKA), cyclin-dependent kinase family (CDK1) and other tyrosine kinase families like ErbB (EGFR) and c-Src.
23. The following abbreviations are used in the descriptions of experimental chemistry procedures: AcOEt, ethyl acetate; AcOH, acetic acid; BOC_2O, di-*tert*-butyl-dicarbonate; DIPE, di-*iso*-propylether; DMF, *N*,*N*-dimethylformamide; FC, flash chromatography; HBTU, (*O*-benzotriazol-1-yl)-*N*,*N*,*N*′,*N*′-tetramethyluronium-hexafluorophosphate; MeOH, methanol; Mp, melting point; NMM, *N*-methyl morpholine; *i*-PrOH, *iso*-propanol; rt, room temperature. All starting materials were purchased from commercial suppliers and used without further purification. Solvents were of reagent grade purity and used as purchased without any additional distillation. FC was performed on Merck silica gel 60 (0.043–0.060 mm). NMR spectra were recorded on a 200-MHz Varian Gemini-200 instrument. Electrospray mass spectra were obtained with a Fisons Instruments VG Platform II. Melting points were recorded on a Büchi model 535 melting point apparatus and are uncorrected. Elemental analyses were performed at Solvias AG, Basel, Switzerland.
24. Synthesis of **4**, 2-*tert*-Butoxycarbonylamino-benzoic acid. To a solution of 40 g (0.292 mol) of anthranilic acid in 1 L of DMF were added 86.6 g (0.397 mol) of BOC_2O and the reaction mixture was stirred at room temperature for 16 h. The solvent was then evaporated, the residue re-dissolved in CH_2Cl_2 and the solution extracted with 10% citric acid and saline. The combined aqueous extracts were twice re-extracted with CH_2Cl_2, the organic extracts combined, dried over Na_2SO_4, and the solvent evaporated. The resulting yellow oil was re-dissolved in CH_2Cl_2 and the product precipitated with DIPE. Reprecipitation from CH_2Cl_2/DIPE gave 33.6 g (48.5%) of the title compound as white crystals. From the mother liquor two additional crops of 3.2 g (white crystals) and 3.9 g (light yellow crystals), respectively, were 155–156 °C. C, H, N (237.26): C 60.71%, H 6.42%, N 5.88%, O 26.72% (calcd C 60.75%, H 6.37%, N 5.90%, O 26.97%). ^{1}H NMR (200 MHz, $CDCl_3$) δ 10.0 (s, 1H); 8.45 (d, 1H); 8.11 (dd, 1H); 7.53 (dt, 1H); 7.04 (dt, 1H); 1.55 (s, 9H).
25. Synthesis of **5**, [2-(4-chloro-phenylcarbamoyl)-phenyl]-carbamic acid-*tert*-butyl ester. To a solution of 33.6 g of **4** (0.142 mol) and 36.2 g (0.283 mol) of *p*-chloro aniline in 660 mL of DMF were added 39.2 mL (0.355 mol) of NMM and 64.3 g (0.170 mol) of HBTU and the reaction mixture was stirred at room temperature for 16 h. The solvent was then evaporated, the residue re-dissolved in CH_2Cl_2 and the solution extracted with 10% citric acid, satd aq $NaHCO_3$, and saline. The aqueous extracts were re-extracted with CH_2Cl_2, the organic extracts combined, dried over Na_2SO_4, and the solvent evaporated. Treatment of the resulting orange-colored oil with CH_2Cl_2 resulted in formation of an orange-colored precipitate, which was discarded. Evaporation of the filtrate, dissolution of the residue in CH_2Cl_2 and precipitation with DIPE gave 16.9 g (35%) of **5** as white crystals. Mp ∼215 °C (dec.). C, H, N (337.81): C 62.23%, H 5.55%, N 8.13%, Cl 10.12%, O 14.23% (calcd C 62.34%, H 5.52%, N 8.08%, Cl, 10.22%, O 13.84%). ^{1}H NMR (200 MHz, DMSO-d_6) δ 10.5 (s, 1H); 9.85 (s, 1H); 8.08 (d, 1H); 7.77 (dt, 1H); 7.75 (d, 2H); 7.52 (dt, 1H); 7.42 (d, 2H); 7.1 (t, 1H); 1.45 (s, 9H). EI–MS: 247 (100% [M−BOC]).
26. Synthesis of **6**, 2-amino-*N*-(4-chloro-phenyl)-benzamide-hydrochloride. To a suspension of 16.5 g (47.6 mmol) of **5** in 660 mL of MeOH were added 40 mL of 4 N HCl/dioxane (N_2-atmosphere). After 30 min a clear yellow solution had formed and after 3.5 h the mixture was concentrated to ca. 50% of its

original volume, resulting in the formation of a white suspension. 500 mL of DIPE were then added and after 30 min the precipitate was isolated by filtration (white crystals). This material was reprecipitated from MeOH/DIPE to yield 13.2 g (97.9%) of **6** as white crystals. ^{1}H NMR (200 MHz, DMSO-d_6) δ 10.5 (s, 1H), 7.8 (m, 3H), 7.65 (s, very broad 3H), 7.45 (m, 3H), 7.10 (d, 1H), 7.08 (t, 1H). EI–MS: 247, 249 ([M + H]).

27. Synthesis of **3**, *N*-(4-Chloro-phenyl)-2-[(pyridin-4-ylmethyl)-amino]-benzamide. To a solution of 0.500 g (1.77 mmol) of **6** and 0.227 g (2.12 mmol) of pyridine-4-carbaldehyde in 8 mL of MeOH were added 80 μL of AcOH and the mixture was stirred at room temperature for 2 h (N_2-atmosphere). After this time $NaCNBH_3$ (0.355 g, 5.65 mmol) was added in several portions and stirring continued for additional 2 h. The solution was then cooled to 0 °C and 100 mL of satd aq $NaHCO_3$ were added. The aqueous solution was extracted with AcOEt (3×) and the combined organic extracts subsequently washed with water (2×), dried over Na_2SO_4 and the solvent evaporated. The residue was purified by FC in CH_2Cl_2/MeOH 30/1 and then recrystallized from hot *i*-PrOH to give 0.200 g (33%) of **3** as white crystals. Mp 134–139 °C. C, H, N (337.81): C 67.1%, H 4.7%, N 12.1%, O 4.9% (calcd C 67.56%, H 4.77%, N 12.44%, O 4.74%). ^{1}H NMR (200 MHz, DMSO-d_6) δ 8.5 (dd, 2H), 7.90 (t, 1H), 7.78 (dd, 2H), 7.70 (dd, 1H), 7.95–7.80 (2×d, 2H + 2H), 7.25 (t, 1H), 6.65 (t, 1H), 6.55 (d, 1H),4.50 (d, 2H).

28. Rialet, V.; Meijer, L. *Anticancer Res.* **1991**, *11*, 1581.
29. Meyer, T.; Regenass, U.; Fabbro, D.; Alteri, E.; Roesel, J.; Muller, M.; Caravatti, G.; Matter, A. *Int. J. Cancer* **1989**, *43*, 851.
30. Mohamadi, F.; Richards, N. G. J.; Guida, W. C.; Liskamp, R.; Lipton, M.; Caufield, C.; Chang, G.; Hendrickson, T.; Still, W. C. *J. Comput. Chem.* **1990**, *11*, 440.
31. (a) 'In-house' addition to Macromodel: Bohacek, R. S.; Guida, W. C. *J. Mol. Graph* **1989**, *7*, 113. (b) Eyraud, V.; Dietrich, A., Novartis Pharma Inc. Unpublished results.
32. Stewart, J. J. P. *J. Comput.-Aided Mol. Des.* **1990**, *1*, 1.